Microscale Thermophysical Engineering, 6:303–317, 2002

1089-3954/02 $12.00 + .00
DOI: 10.1080/10893950290098340

Taylor & Francis
Taylor & Francis Group

THERMOFLUID DYNAMIC STUDY OF FLAT-PLATE CLOSED-LOOP PULSATING HEAT PIPES

S. Khandekar, M. Schneider, P. Schäfer, R. Kulenovic, and M. Groll

Institut für Kernenergetik und Energiesysteme (IKE), Universität Stuttgart, Stuttgart, Germany

Meandering-tube pulsating heat pipes (PHPs) have already found some applications in cooling power/microelectronic components. Reliable experimental data for PHPs is very limited, especially in the wake of the ongoing miniaturization process and efforts to combine electronic components and heat spreaders on the chip level. In fact, the basic operation of PHPs is far from being fully understood, and there are no available design tools for given microelectronics cooling requirements.

A logical next step for further applications of PHPs in microelectronics cooling is to design integral structures, i.e., PHPs as an integral part of thermal spreader/substrates, having typical dimensions as applicable for multichip modules or printed circuit boards (PCBs). In this article, experimental results for flat-plate, closed-loop PHP structures (rectangular and circular, $D_{hyd} \approx 2.0$ mm) which are integrally machined into an aluminum substrate (115 × 36 × 3 mm^3) and covered by a glass plate for visualization are presented. Working fluids employed are water and ethanol. To verify certain observed phenomena, another PHP setup is made consisting of 10 glass tubes (ID 2.0 mm) connected by copper U-turns. As input parameters, fill rate, heat load, and tilt angle are varied. Axial temperature distribution is recorded with thermocouples. By means of a high-speed video camera and a thermo-camera, the evaporation/condensation processes and the individual liquid–vapor plug characteristics are studied. The results enable explanations for operational characteristic and performance limits, which are influenced by capillary resistance, gravity, and thermofluid dynamic effects. Preliminary design rules are also discussed.

Pulsating heat pipes [1, 2] are potentially cheaper than conventional wicked heat pipes. Although conventional heat pipes (mini or micro) are one of the proven technologies, the manufacturing of the complex, miniaturized wick structure/geometry of these heat pipes could be the most cost-intensive factor, along with the heat pipe material itself. Recent trends in microelectronics have shown the limitations of conventional designs [3]. Since no wick is needed in a PHP, one-step drawing, bending, machining, or etching for a wide range of materials seems to be possible.

A closed-loop pulsating heat pipe consists of tubes/channels of capillary dimensions arranged in a serpentine manner and joined end to end as shown in Figure 1*c*. It is first evacuated and then filled partially with a working fluid, which distributes itself naturally

Received 23 July 2001; accepted 1 July 2002.
Address correspondence to Sameer Khandekar, Institut für Kernenergetik und Energiesysteme (IKE), Universität Stuttgart, Pfaffenwaldring 31, 70550 Stuttgart, Germany. E-mail: khandekar@ike.uni-stuttgart.de

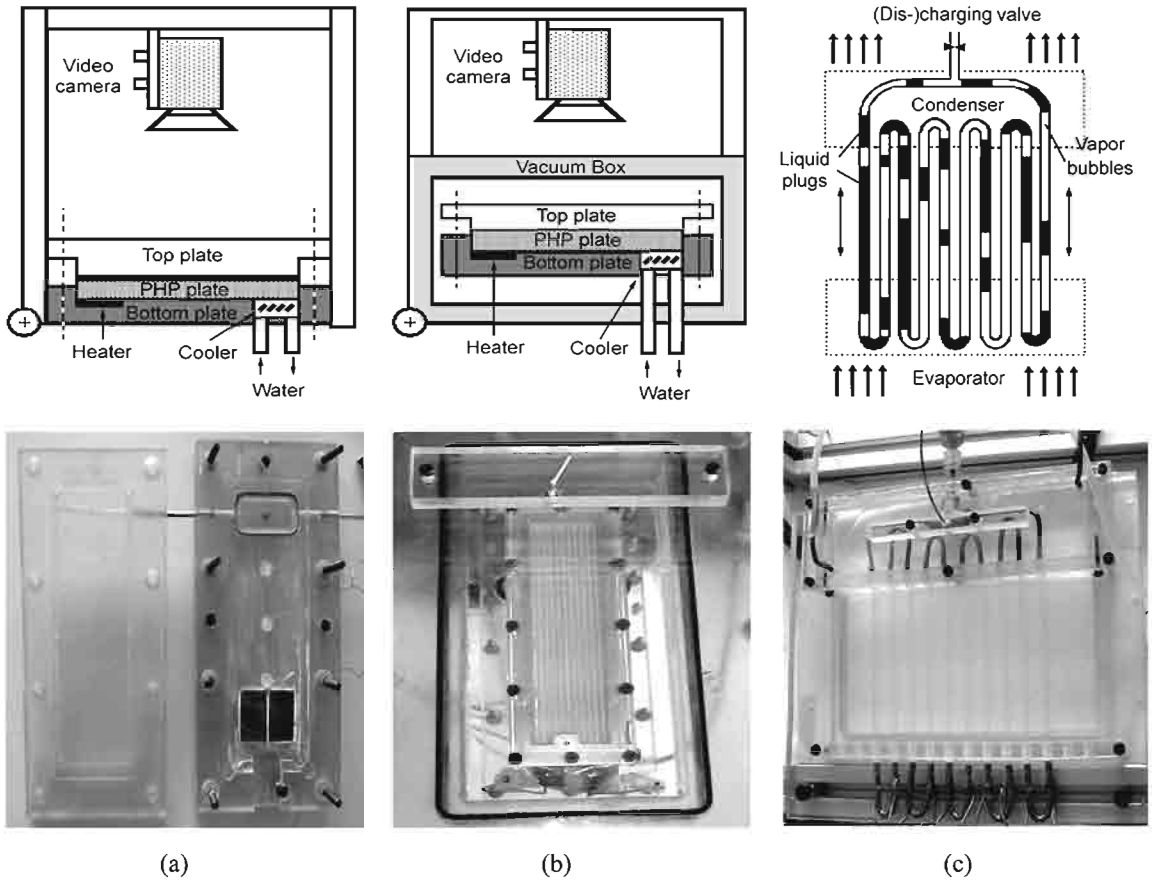

Figure 1. (*a*) Sandwich setup. (*b*) Vacuum box setup. (*c*) Glass tube setup.

NOMENCLATURE

D	diameter, m	ρ	mass density, kg/m^3
g	acceleration due to gravity, m/s^2	σ	surface tension, N/m
P	pressure, Pa		
Q	heat transfer rate, W	**Subscripts**	
R	thermal resistance, K/W	cap	capillary
T	temperature, K	hyd	hydraulic
r	radius, m	i	inside
α	wetting angle	l	liquid
λ	thermal conductivity, W/m K	v	vapor

inside in the form of liquid–vapor plugs and slugs. One end of this structure receives heat, transferring it to the other end by a pulsating action of the liquid–vapor system. There may exist an optional adiabatic zone in between. A PHP is essentially a nonequilibrium heat transfer device, performance success of which primarily depends on the continuous maintenance or sustenance of these nonequilibrium conditions within the system. The liquid–vapor slug transport is due to thermally driven pressure pulsations in the respective tubes. No external power source is required for fluid transport as in the case of DREAM pipes [1, 3].

1. DESCRIPTION OF EXPERIMENTS

1.1. Description of Experimental Setups

Three different setups are built for the experiments. Setups one and two (Figures 1*a* and 1*b*) are designed for thermal and optical investigations on flat aluminum plate PHPs. Setup three (Figure 1*c*) is made of glass tubes interconnected by copper U-turns and is designed as a verification setup. In order to study the influence of gravity on the device performance and oscillating patterns, each setup can be tilted in a range from 0° (horizontal) to 90° (vertical). In vertical orientation, the heater is always located below the cooler.

Setup one consists of two polycarbonate plates (top and bottom) with the PHP clamped in between. At one end an electrical heater is integrated into the bottom plate. A water cooler, cavity machined in the base plate, is located at the other end. The surface temperature profile of the PHP is measured by means of five thermocouples, located on the same side as the heater and cooler. One thermocouple is at the heater center, three are in the adiabatic section, and one is in the cooler section. The heater and cooler have effective areas of $3.0 \times 2.25 = 6.75$ cm^2 and $3 \times 1.35 = 4.05$ cm^2, respectively, with the effective distance between them being 95 mm. The PHP consists of an aluminum plate ($130 \times 45 \times 3$ mm^3) with integrated longitudinal interconnected grooves covered by a transparent glass or polycarbonate plate (thickness each = 3.0 mm), kept leak tight by an O-ring seal and anchored by screws in the bottom plate. The size of this plate is of the same order as the mini-heat pipe arrays developed during the BRITE-EURAM project "Khiepcool" [4]. These supplementary structures (O-ring fixture, glass plate, etc.) increase the effective cross-sectional area so that the overall thermal resistance is lower

than that of the bare aluminum structure. The oscillations of the liquid–vapor plugs are recorded by a high-speed video camera, fixed on the same tiltable frame as the PHP module and thus ensuring the same top view at all angles.

Setup two (Figure 1*b*) is very similar to setup one with regard to the test PHP structure, electrical heater, the cooling technique, and the common frame. The main difference is the use of a vacuum box enclosure enabling accurate quantitative measurements. However, the aluminum support frame decreases the thermal resistance of the test structure even more than in the case of setup one. In the case of a PHP with circular channels, one half of the channel is machined into the aluminum base and the other into the polycarbonate cover. The areas of the heater plate and the condenser cavity are $3.1 \times 2.95 = 9.15$ cm^2 and $2.0 \times 2.8 = 5.6$ cm^2, respectively with the effective distance between them being 95 mm.

Setup three consists of 10 parallel glass tubes (ID 2.0 mm, OD 4.2 mm, length 10.0 cm, inter-tube axis distance 12.0 mm) interconnected alternately by copper U-turns (ID 2.0 mm) which are joined by silicon tubing. A (dis-) charging valve is attached to the outermost two tubes with a T-part forming the closed loop as shown. Resistance heater wires wrapped around the copper U-turns on one side form the evaporator. The copper U-turns of the other side are routed through a cooling box supplied by isothermal coolant water. The heater U-turn height is 25 mm and the cooler U-turn height is 20 mm.

Altogether, six experiments were performed (see Table 1). Experiments 1–4 were supposed to be quantitative experiments in order to find optimum fill charges and minimum thermal resistance. The last two experiments (with the glass tube PHP setup) were done to verify qualitatively some hypotheses based on the results of tests 1–4. The inner PHP channel/tube hydraulic diameters were always as suggested in the literature [1]:

$$D_i \leq 2 \cdot \sqrt{\frac{\sigma}{g \cdot (\rho_l - \rho_v)}} \tag{1}$$

Table 1. *Details of experiments*

Setup	Exp. no.	Channel type/ cross section	Channel length	No. of channels	Inter-channel axis distance	Heater area	Cooler area	Tested fluid
#1	1	Rectangular 2.2×2 mm^2	104 mm	12	2.5 mm	7.0 cm^2	4.0 cm^2	Water
#2	2	Rectangular 1.5×1 mm^2	104 mm	12	2.5 mm	9.0 cm^2	5.6 cm^2	Water
	3							Ethanol
	4	Circular ID 2.0 mm						Water
#3	5	Circular	145 mm	10	12 mm	*[a]	*[a]	Water
	6	ID 2.0 mm				*[a]	*[a]	Ethanol

[a] Approximately 60-mm heater length per single U-bend (total bends = 5); approximately 50-mm cooler length per single U-bend (total bends = 4); closed-loop location always in the cooler.

1.2. Measurement Procedure

For all three kinds of setups with water as working fluid, the PHPs were first evacuated (vacuum $< 10^{-4}$ mbar) and then filled completely with distilled, deionized, and degassed water. For practical reasons, this method was not applicable to ethanol. Hence, ethanol was filled in through the charging valve, displacing the air through a seal, which was kept loose, until the whole system was filled with ethanol. Later the desired quantity of ethanol could be sucked out.

For flat-plate PHPs the thermal resistance of the empty structures was measured before charging to obtain reference values.

After the PHP was completely filled, it was put in the vertical orientation (heater below cooler). The fill charge was then reduced by some percent and the heat input was stepwise increased until the evaporator tubes showed a steady (average) temperature of 120°C (maximum safe operation). Thus the maximum heat throughput for safe operation at a given fill charge was obtained. The fill charge was then reduced and the above procedure repeated. In this way a set of points representing maximum heat throughputs at respective fill charges was obtained, from which the optimum fill charge could be evaluated. For each power and fill charge step, the system was tilted until the point of drastic increase of the thermal resistance was reached. Thus the critical tilt angle was measured.

For temperature measurements, a data logger (resolution 0.1°C, accuracy ±0.5°C, time constant of 70 ms) was employed with a measuring frequency of 1 Hz, coupled with ungrounded K-type thermocouples (Thermocoax) of 1 mm diameter. The thermocamera was always calibrated with standard emitting surface compared to the actual reading of thermocouple placed on it. A worst-case analysis (for setup #1) indicates that the accuracy of measurement for maximum heat throughput is below 7%. The results indicated in the next section are averaged-out indicative values of a series of test repetitions. For the glass-copper tube PHP (setup #3), only qualitative results are of importance.

2. THERMAL AND VISUALIZATION RESULTS

Table 2 shows the main results of the thermal measurements. The last two rows show the calculated thermal resistance for equivalent solid/bare aluminum and copper plates, respectively. Due to the additional supporting frame of the setup modules, the

Table 2. Thermal performances of flat-plate PHPs

Setup No./ Exp. No.	Q_{max} (W), vertical	Q_{max} (W), horizontal	R_{empty} (K/W)	$R_{overall}$ (K/W), vertical	$R_{overall}$ (K/W), horizontal	$R_{PHP\ effect}$ (K/W), vertical	Fill rate (%)	Critical angle (deg)
#1/1	70	N/A	7.2	1.1	>4.0	1.3	<10	5–15
#2/2	45	N/A	4.8	2.0	>4.0	3.5	30	5–15
#2/3	45	N/A	4.7	2.0	>4.0	3.4	25	5–15
#2/4	25	N/A	4.1	1.8	>4.0	3.1	70	5–10
Solid Al	—	—	5.2	—	—	—	—	—
Solid Cu	—	—	2.6	—	—	—	—	—

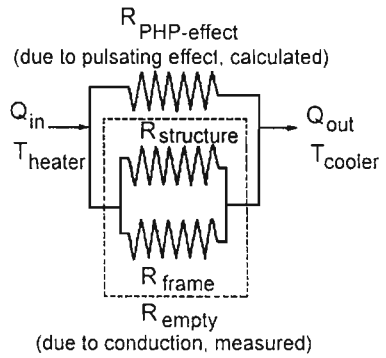

$$R_{overall} = (T_{heater} - T_{cooler})/Q_{in} \tag{2}$$

$$R_{PHP-effect} = \left(\frac{1}{R_{overall}} - \frac{1}{R_{empty}} \right)^{-1} \tag{3}$$

Figure 2. Thermal resistance model of the metal PHP.

"empty" thermal resistances of experiments 2, 3, and 4 are smaller than that of a solid aluminum plate. This influence is very pronounced for setup #2, where the thermal resistance of an empty structure is remarkably smaller than that of the setup #1 structure. Column 7 shows the theoretical thermal resistance due to "pure" PHP effect. Considering the heat being conducted through two parallel thermal resistances (solid material and pulsating effect, see Figure 2), these PHP resistances are calculated as shown in Figure 2.

2.1. Vertical Operation

In vertical operation the thermal resistances show acceptable values only for experiment 1 (see Table 2 and for explanation refer to Section 3.2). Regarding the PHP-effect resistance, it is obvious that in this case the heat is mainly transferred by pulsating effect and not by pure conduction. However, for the other experiments the part of nonconductive heat transfer is much smaller, hence there seems to be no advantage to such a PHP plate compared to a solid copper plate.

Regarding the impact of the cross section and fill rate on the thermal resistance and maximum heat transport capability, it was found that:

The structures with the larger D_{hyd} (2 mm) show the highest heat throughput at the lowest thermal resistance (rectangular grooves).

The thermal resistance of a structure with rectangular cross section is lower than that of one with circular cross section although both have the same hydraulic diameter (Exp. 1 and Exp. 4).

The structure with circular cross section has the lowest heat transport capability (but a small thermal resistance).

For circular cross sections, the optimum fill rate is the highest.

For rectangular sections, the optimum fill rate is close to that of an axially grooved heat pipe (<30%).

A correlation of the visual observations with the thermal measurements revealed obvious dependencies on fill rate, heat load, working fluid, and cross-section geometry. For fill rates >25% and water as working fluid, two different phases of operation were

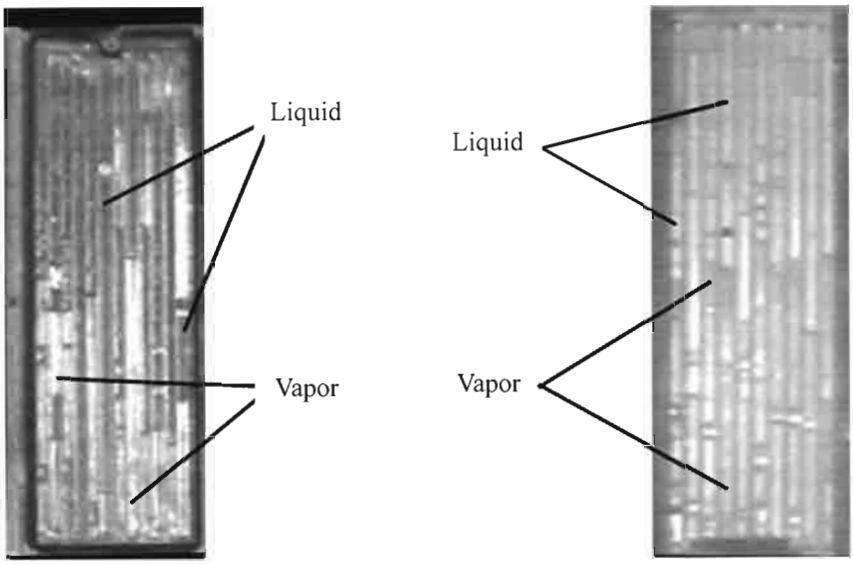

Figure 3. (*a*) High-speed video camera picture of a 2.2 × 2.0 mm^2 PHP structure in vertical orientation in oscillation phase (fill rate 50%, Q_{in} = 70 W). (*b*) Picture of a circular-cross-section PHP structure in vertical orientation in static phase (fill rate 50%, Q_{in} = 45 W). Most liquid is collected in the cooler area.

recorded. Oscillations occurred only for short time periods ("oscillation phase," about 2 s, see Figure 3*a*) and then stopped for several seconds (about 10 s, "static phase"). In the static phases, boiling could be seen in the heater zone (generation of bubbles), while more and more liquid collected in the cooler area (see Figure 3*b*). Further, the temperature difference between heater and condenser increased by a few degrees. In the oscillation phase several types of moving liquid plugs and bubbles were recorded. At the same time the temperature difference decreased. These plug and bubble types were also observed in the glass tube verification experiments. The alternating "static" and "oscillating" phases continued throughout the experiments.

For the rectangular grooves, a fill charge decrease eventually led to the complete disappearance of almost all distinct liquid plugs while the thermal resistance continued to decrease. Finally, almost no liquid plugs remained and liquid was only visible in the channel edges. The surface temperature profile indicates (see Figure 4), that for very small fill rates (about 10%) the adiabatic section becomes isothermal. The grooves obviously operate as capillary-assisted thermosyphons and not in the real pulsating heat pipe mode. In this case, almost no liquid plugs blocked the vapor flow from heater to condenser. For higher fill rates (about 70%), a sizable temperature gradient was measured. A fill rate reduction below 10% caused dry-out and thus a drastic increase of the thermal resistance.

A two-phase thermosyphon effect, as noted above for the rectangular grooves, could not be seen for the circular-cross-section PHPs, as no sharp edges were present which could act as capillary structures. However, the effect of periodic oscillation phases followed by much longer static phases with nucleate-type pool boiling in the heater area was recorded in this case too.

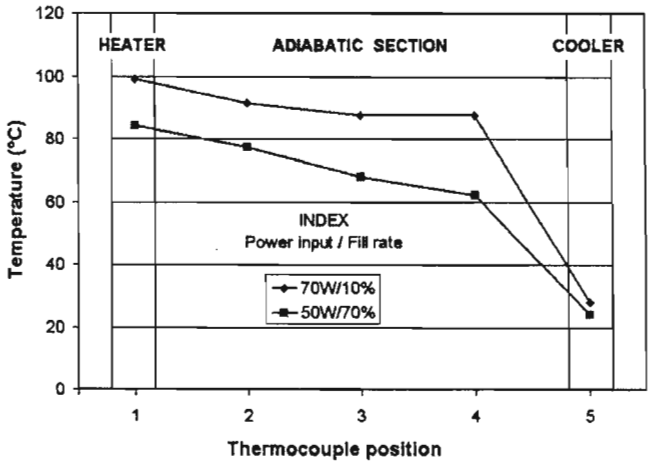

Figure 4. Average temperature profile of vertical PHP (setup #1, Exp. 1).

2.2. Horizontal Operation

Close to *horizontal orientation* (between 5° and 15° to horizontal), any kind of oscillations stopped completely, the heater area dried out, and the thermal resistance increased drastically to a value of the order of the reference empty structure resistance (>4.0 K/W). The plates could not be operated for heat loads exceeding about 10 W (safe limit), hence a reasonable thermal resistance could not be measured. After restoring the tilt angle above the *critical angle*, the operation restarted. Ethanol had smaller critical angles (stopping and restarting), but of the same order as those of water. In any case, proper operation was not achieved for horizontal orientation in the present series of experiments.

3. EXPLANATIONS FOR UNSATISFACTORY PERFORMANCE

3.1. Transverse Heat Balancing Effects

Due to the very thin wall between two neighboring channels in the investigated metal structures, the transverse thermal resistances are very low (for a 1-cm-long wall segment, with area $A = 22$ mm^2, thickness $w = 0.5$ mm; $R_{\text{wall}} = w/A \cdot \lambda_{\text{Al}}) = 0.114$ K/W). This results in high heat transfer rates between two plugs with different temperatures in adjacent channels (see Figure 5). This phenomenon quickly equalizes the thermally created pressure gradients, the primary driving potential for proper PHP operation. This hypothesis leads to the first conclusions that for a proper operation of a flat aluminum plate PHP:

A suitable fluid should have a larger $(\partial P/\partial T)_{\text{sat}}$ than water or ethanol, thereby creating large pressure fluctuations with smaller heat input.
As far as possible, the heat transfer between the channels must be reduced.

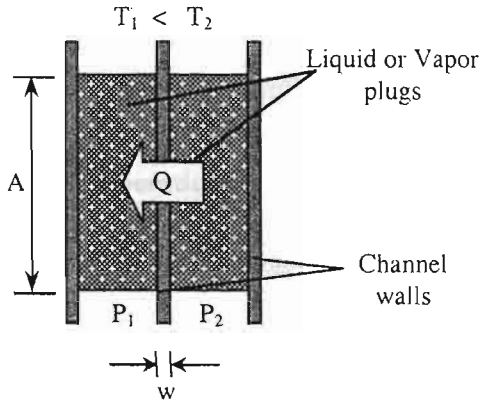

Figure 5. Temperature/pressure balancing across adjacent channels.

3.2. Sharp-Angled Edges

The sharp-angled edges of a channel act as capillary structures. This influence, when coupled with gravity assistance, certainly enhanced the heat transport capability and reduced the thermal resistance at lower fill rates. In such cases the device functioned as a gravity-assisted thermosyphon. However, this effect is negligible for high fill charges, where several liquid plugs prevent a direct vapor flow from the heater to the condenser.

3.3. Capillary Resistance due to Dynamic Contact Angle Hysteresis

Certain liquid/solid combinations under capillary slug flow conditions encounter an additional friction, the "capillary resistance." This resistance is due to the capillary pressure difference between the plug front (in the moving direction) and the plug end (against movement). The difference is caused by different curvatures, an effect of dynamic contact angle hysteresis [5]. The trailing plug curvature slips over a just-wetted surface by the bulk liquid, while the front meniscus has different conditions (Figure 6). Thus, applying the Laplace equation for capillary pressure gradient across a liquid–vapor interface in a tube of circular cross section,

$$F_{\text{cap}} = 2\pi \cdot r_i \cdot \sigma \cdot (\cos \alpha_{\text{front}} - \cos \alpha_{\text{back}})|_{\text{dynamic}} \tag{4}$$

For water/glass, $\alpha_{\text{front}}|_{\text{dynamic}} \approx 80°$ and $\alpha_{\text{back}}|_{\text{dynamic}} \approx 42°$, were measured, i.e., a single water plug ($\sigma = 0.072$ N/m at 25°C) in a glass tube ($r_i = 0.001$ m) has to overcome an additional capillary resistance force of $F_{\text{cap, water}} = -0.26 \times 10^{-3}$ N. For ethanol the two dynamic contact angles were about the same and less than 10°. Therefore, in this case the additional resistance is negligible. This additional resistance is additive and is amplified if several plugs are simultaneously located in a channel (Figure 7). These cumulative pressure gradients thwart oscillations and therefore fluid/solid combinations having large dynamic contact angle hysteresis should be avoided.

3.4. Effect of Latent Heat

The rate of growth of bubbles formed in the heater area is inversely proportional to the latent heat. A sudden growth causes pressure pulses that excite oscillations. As long

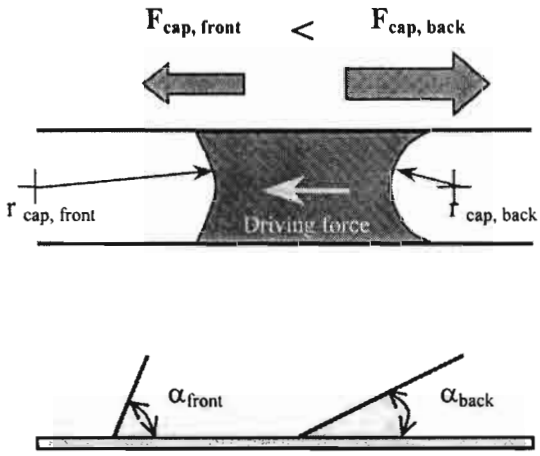

Figure 6. Capillary resistance due to dynamic contact angle hysteresis.

as one vapor–liquid interface is in the heater area, the bubble continues to grow. This is valid with opposite effect in the cooler area.

For fluids having very small latent heat the bubble sizes in the heater area rapidly increase. Thus there is a possibility of the whole fluid (liquid phase) collecting in the condenser area. Moreover, it can also happen that a bubble gets too large for the heater area and thus no vapor–liquid interface is present for taking up heat. Thus, the heater temperature increases until the entire amount of fluid entering the heater area is immediately vaporized. However, this effect can be suppressed by adjusting the fill charge. If the latent heat is too large, the rate of change of bubble volume will be small, resulting in insufficient pressure pulses, leading to reduced oscillations.

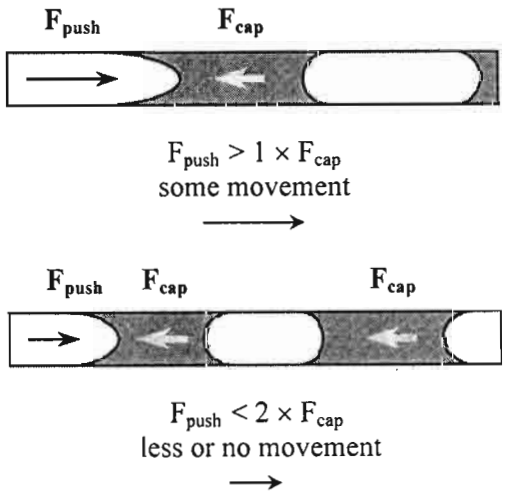

Figure 7. Influence of several plugs in a tube on resistance to movement.

4. VALIDATION EXPERIMENTS WITH GLASS TUBE PHP SETUP

Some of the hypotheses could be proven by means of the glass tube setup three with experiments 5 and 6 (see Table 1).

4.1. Operation Modes

With water as working fluid, unlike ethanol, the glass PHP does not operate in horizontal orientation, but only in vertical orientation. For ethanol, although the tilt angle affects the temperature gradient between heater and cooler, satisfying operation is possible for both orientations. As in the case of flat-plate PHPs, static and oscillating phases alternate, but the frequency is much higher.

4.2. Capillary Resistance

In Figure 8 the difference of contact angles across liquid plugs for the two working fluids is shown. For water, a distinct difference in leading and lagging contact angles is seen, whereas the ethanol liquid plugs/bubbles show no such difference. It was frequently observed that the global positions of the water plugs in the whole PHP do not change, but only the interface curvatures oscillate due to alternating effective pressure on the bubble. For ethanol such behavior was not found. Together with the fact that water does not allow horizontal operation, it is evident that the dynamic contact angle hysteresis plays an important role.

4.3. Intertube Heat Balancing

The temperature difference between the tubes of a properly operating PHP (ethanol) can be seen in Figure 9. A typical average intertube temperature difference is of the order of 15–20 K for vertical orientation and a heat load of 45 W. For horizontal orientation the temperature difference is increased up to 45 K at a heat load of 20 W.

The average intertube temperature difference indicates a directed mass flow, although the videos do not show directed oscillation patterns of the bubbles. This means that the bubbles frequently replace liquid (i.e., liquid flows through the thin film around the bubble) rather than pushing liquid plugs. Only for horizontal orientation can a visible dependency between vapor bubbles and temperature be seen. In this case, the colder tubes are completely free of bubbles, whereas the hot ones contain bubbles (see also Figure 8, ethanol). However, the flow direction is alternating, with a period of several tens of seconds, as can be seen in Figure 10. The obvious fact that an intertube temperature difference is observed supports the hypothesis that a minimum intertube temperature difference is needed for proper operation.

5. SUMMARY AND CONCLUSIONS

It was investigated whether a flat-plate, closed-loop pulsating heat pipe can be applied for microelectronics cooling from chip to heat sink.

The measured thermal resistances were strongly influenced by the tilt angle, fill rate, and cross-sectional geometry. The best performance of the PHPs with rectangular

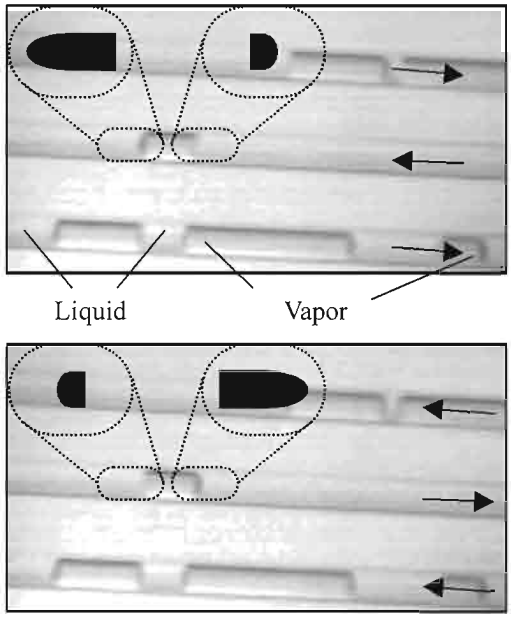

Water: Depending on the moving direction, the bubble curvatures change

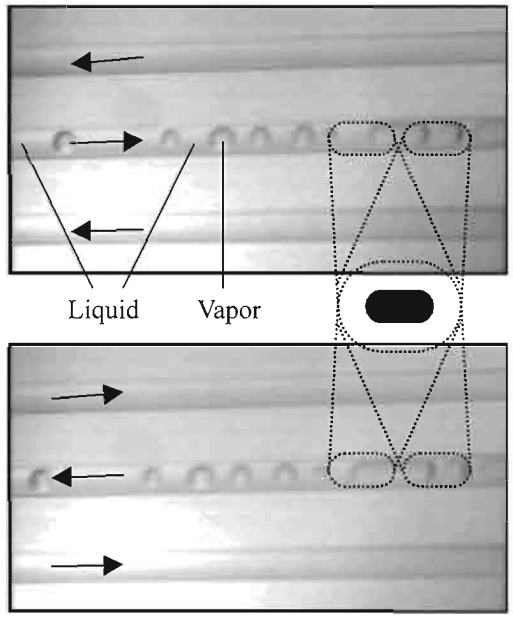

Ethanol: No directional dependency of the curvatures.

Figure 8. Contact angle hysteresis of the moving bubbles (both cases in horizontal orientation with heat input of 20 W).

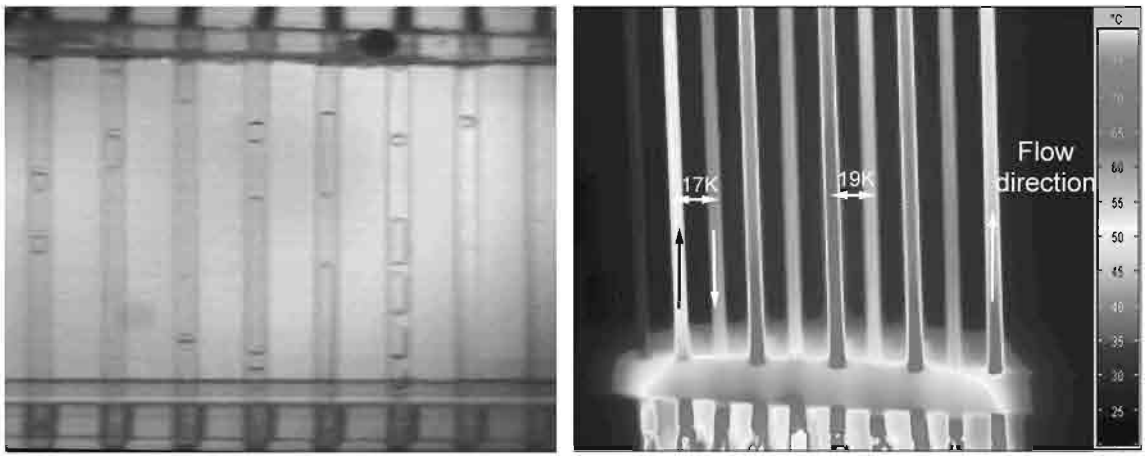

Figure 9. High-speed picture and thermograph of a properly operating PHP (ethanol, vertical, $Q_{in} = 45$ W, fill rate 70%).

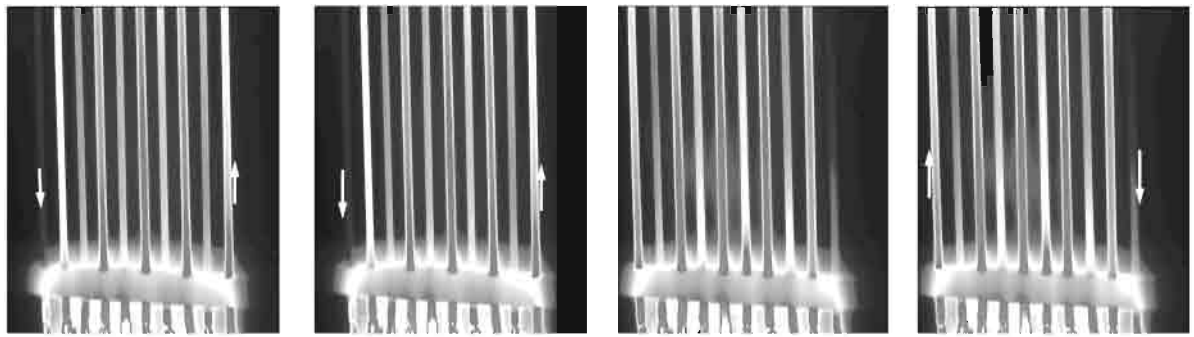

Figure 10. Alternating flow direction in a vertical PHP. After 20 s, macro-level movements stop and flow begins in the opposite direction (ethanol, $Q_{in} = 45$ W, fill rate 70%).

cross section was observed with fill rates less than 10% in vertical orientation. In these cases the fluid was mainly transported in the channel edges, i.e., the grooved plate worked as a capillary-assisted thermosyphon rather than as a PHP. A thermal resistance of about 1 K/W could be obtained for a 2.2×2.0 mm^2 rectangular-cross-section PHP. The maximum heat throughput was 70 W.

The circular-cross-section PHP had the lowest maximum heat throughput, and the thermal resistance (1.8 K/W) was not much better than that of an equivalent solid copper plate (2.6 K/W). A capillary-assisted thermosyphon operation mode was not found in this case, and the optimum fill ratio was about 70%. In horizontal orientation none of the metallic PHPs worked satisfactorily. The oscillations stopped completely and the thermal resistance became similar to that of an empty structured plate. Verified with a glass PHP setup and by means of a thermo-camera, the following three preliminary design criteria are identified:

1. A fluid should have a large $(\partial P/\partial T)_{\text{sat}}$, in any case larger than that of water or ethanol.
2. Fluid–solid combinations with negligible contact angle hysteresis should be preferred.
3. As far as possible, the transverse heat interactions between the channels must be reduced.

Consequently, it was found that the typical PHP concept could only be applied with strong reservations for a flat-metal-plate PHP with water or ethanol as the working fluid.

REFERENCES

1. H. Akachi, F. Polášek, and P. Štulc, Pulsating Heat Pipes, *Proc. 5th Int. Heat Pipe Symp.*, Melbourne, Australia, pp. 208–217, 1996.
2. H. Akachi and Y. Miyazaki, Stereo-Type Heat Lane Heat Sink, *Proc. 10th Int. Heat Pipe Conf.*, Stuttgart, Germany, 1997.
3. S. Nishio, Attempts to Apply Micro Heat Transfer to Thermal Management, *Proc. Int. Conf. on Heat Transfer and Transport Phenomena in Microscale*, Banff, Canada, pp. 32–40, 2000.
4. C. Sarno, J. Dezord, G. Moulin, M. Zaghdoudi, M. Lallemand, V. Sartre, M. Groll, M. Schneider, H. Holzer, T. Schmitt, J. Rantala, T. Aapro, and R. Lehtinimi, Use of Metal Matrix Composite Material Heat Pipes for the Thermal Management of High Integrated Electronic Packages, *Proc. 11th Int. Heat Pipe Conf.*, Tokyo, Japan, 1999.
5. V. P. Carey, *Liquid–Vapor Phase Change Phenomena*, pp. 76–83, Hemisphere Publishing Corporation, 1992.